Replication of the Enzymatic Temperature Dependency of the Primary Hydride Kinetic Isotope Effects in Solution: Caused by the Protein Controlled Rigidity of the Donor-Acceptor Centers?

Yun Lu,* Samantha Wilhelm,† Mingxuan Bai,† Peter Maness, Li Ma

Department of Chemistry, Southern Illinois University Edwardsville, Edwardsville, Illinois 62026, United States

Supporting Information Placeholder

ABSTRACT: The change from temperature independence of the primary (1°) H/D kinetic isotope effects (KIEs) in wild-type enzyme catalyzed H-transfer reactions ($\Delta E_a = E_{aD} - E_{aH} \sim 0$) to strong temperature dependence with the mutated enzymes ($\Delta E_a >> 0$) have recently been frequently observed. This has prompted some enzymologists to develop new H-tunneling models to correlate ΔE_a with the donor-acceptor distance (DAD) at the tunneling-ready state (TRS) as well as the protein thermal motions/dynamics that sample the short DAD_{TRS}'s for H-tunneling to occur. While evidence supporting or disproving the thermally activated DAD sampling concept has extensively emerged, comparable study on the simpler bimolecular H-tunneling reactions in solution has not been carried out. Especially, small ΔE_a's (~ 0) have not been found. In this paper, we report a study of the hydride transfer reactions from four NADH models to the same hydride acceptor in acetonitrile. The ΔE_a's were determined, which are 0.37 (small), 0.60, 0.99, and 1.53 kcal/mol (large), respectively. The α-2° KIEs on the acceptor that serve as a ruler for the rigidity of reaction centers were either previously reported or determined. All possible productive reactant complex (PRC) configurations were computed to provide insight into the structures of the TRS's. Relationships among structures, 2° KIEs, DAD_{PRC}'s, and ΔE_a's were discussed. The more rigid system with more suppressed 2° C-H vibrations at the TRS and more narrowly distributed DAD_{PRC}'s in PRCs gave a smaller ΔE_a. Results replicated the trend observed in enzymes versus mutated enzymes, and appeared to support the concepts of different thermally activated DAD_{TRS} sampling processes in response to the rigid versus flexible donor-acceptor centers.

Introduction

Recent understanding of the enigmatic enzymatic rate enhancement has been partly shifted from how enzymes organize their active site to stabilize the transition state (TS), to how enzymes' local fast dynamics dictate the activated reaction centers transiently moving to reach their nearest contact for chemistry to occur.[1-8] The latter refers to an activation process in which protein dynamics (or vibrations, heavy atom motions) regulate the donor-acceptor distances (DADs). Searching for this physical origin of enzyme catalysis is an important contemporary research field. It has attracted tremendous attention of enzymologists as well as chemists and physicists. However, whether there is such an origin and ways that researchers use to identify it are currently hotly debated. Nevertheless, information gained about the role of enzyme dynamics in catalysis, if any, would benefit the design of efficient biocatalysts, inhibitors as well as drugs.

One strategy to study the role of fast protein dynamics in catalysis uses enzymes that catalyze the H-tunneling reactions in which H tunnels through the energy barrier due to its wave properties.[9-11] This has been based on the contemporary vibrationally assisted activated H-tunneling (VA-AHT) model (also called the Marcus-like H-tunneling model). That model links the primary (1°) H kinetic isotope effect (KIE) to the H-donor-acceptor distances (DADs) and correlates the heavy atom motions (from protein, substrate and cofactor) with the sampling of short DADs for efficient H-tunneling to occur at the tunneling ready states (TRSs).[9,12-15] Over the past 20 years, it has been frequently observed that the 1° KIEs are temperature independent or weakly temperature dependent in the wild-type enzymes (*wt*-enzymes), whereas they become temperature dependent to various extents in their mutated forms (*mut*-enzymes).[2,12,16-23] Within the VA-AHT model, the weak temperature dependence of the 1° KIEs can be explained in terms of well-organized reaction coordinate in which the DAD_{TRS} is short and the range of the fluctuating DAD_{TRS}'s is narrow, implicating that the wild-type enzymes have strong compressive vibrations that press the two reactants close to each other prohibiting them from being separated. In *mut*-enzymes, the naturally evolved compressive vibrations are impaired, the average DAD_{TRS} becomes longer and the DAD_{TRS} sampling range becomes broader. That is, the *mut*-enzymes do not have as short DADs and strong vibrations (or high rigidity) as in the densely packed active site of the wild-type enzymes that facilitate the sampling of the short tunneling DAD_{TRS}'s.

Computational simulations of the temperature dependency of 1° KIEs have been carried out following various theoretical models to support or disprove the role of the fast thermal motions in sampling short DAD_{TRS}'s for catalysis. These include the quantum mechanical and molecular mechanical (QM/MM) calculations, and sometimes gas-phase DFT calculations, using the nonadiabatic vibronic model of H-tunneling (one form of the VA-AHT model),[24-26] or the ensemble averaged variational TS theory with multi-dimensional H-tunneling (EA-VTST/MT),[27-29] or the empirical valence bond (EVB) theory[5,30,31]. While the nonadiabatic H-tunneling models appeared to be able to reproduce the temperature dependency of the 1° KIEs observed in the *wt*-enzymes versus *mut*-enzymes to support the thermally activated DAD

sampling concept,[12,15,24,32,33] theoretical replications of the observations using other H-tunneling models, especially for the huge 1° KIEs, have encountered difficulty.[27,33-35] Nevertheless, even some of the latter computational results sometimes show that the weak temperature dependence of the 1° KIEs results from the insensitivity of the DAD_{TRS}'s to temperature,[24,28,31,36] whereas other researchers have shown that it could also result from the effect of temperature on the microscopic mechanism, for example, on the position of the TS and the shape of the potential barrier.[27,31]

We regard that ideas about the correlations of the temperature dependence of the 1° KIEs with the DAD sampling in enzymes could be tested by study of the simpler reactions in solution, for which DADs could be controlled by structures. Our purpose is thus to design H-transfer reactions in solution in an attempt to study the relationship between structures/DADs and temperature dependency of the 1° KIEs. The latter relationship has not been investigated before as none of the previous H-transfer models prior to the VA-AHT theory predicts any form of it. Our design uses the hypothesis on the basis of the above explanations; *i.e.*, wild-type enzymes possess narrowly distributed short DAD_{TRS}'s that correspond to the weak temperature dependence of the 1° KIEs, and *mut*-enzymes have broadly distributed long DAD_{TRS}'s that correspond to the strong temperature dependence of the 1° KIEs. The hypothesis is that the more rigid the reaction system, the harder for the DAD_{TRS} to change with temperature (corresponding to a narrower DAD_{TRS} range), the weaker the temperature dependency of the 1° KIEs will be (Scheme 1). Here a rigid TRS can be a tightly associated one with strong electronic interactions/attractions between donor and acceptor, and/or with steric factors that minimize the flexibility of the two reaction centers. This study provides insight into the role of protein thermal motions in catalysis and opens a new physical organic chemistry research direction that studies the relationship between structure and temperature dependency of the 1° KIEs in general H-transfer reactions.

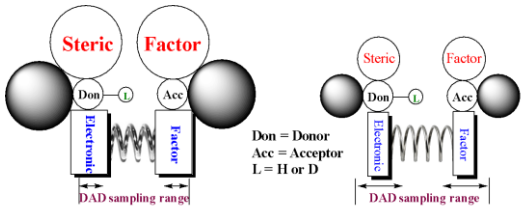

Scheme 1. We hypothesize that the more rigid the H-transfer reaction centers, the more narrowly distributed the donor-acceptor distances (DADs), the weaker the temperature dependence of the 1° KIEs. Two factors are used to control the rigidities of the reaction centers, electronic and steric effects. The larger circles are used to describe a greater crowding effect. The thicker spring and larger rectangles represent a stronger donor-acceptor electronic interaction. The double-headed arrows represent the DAD fluctuation magnitudes determined by the donor-acceptor center rigidities.

In this paper, hydride transfer reactions of NADH/NAD^+ analogues were designed to investigate the hypothesis. They use four distinctively different hydride donors, the same hydride acceptor, and acetonitrile as the solvent. The hydride donors are 1-benzyl-1,4-dihydronicotinamide (BNAH), diethyl 1,4-dihydro-2,6-dimethyl-3,5-pyridinedicarboxylate (Hantzsch ester, HEH), 1,2,3-trimethylbenzimidazoline (TMBIH), and 1,3-dimethyl-2-phenylbenzimidazoline (DMPBIH), respectively. The hydride acceptor is N-methylacridinium ion ($MA^+BF_4^-$). These have been described in eqn (1). We regard that the rigidity will increase from the system of BNAH to that of HEH. This is because in addition to

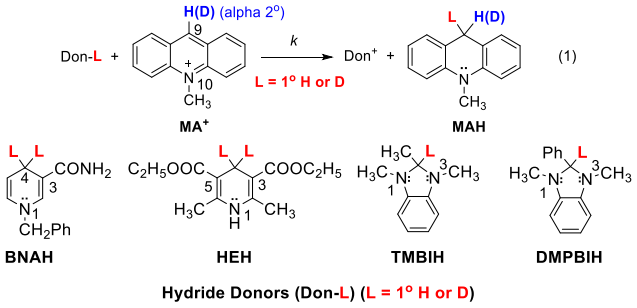

the same 1,4-dihydropyridine moiety that can form π-π stacking interaction with the MA^+, HEH has two ester carbonyl groups at the C-3,5 positions, which can interact with the MA^+ ring through the n-π interaction and/or other types of polar-polar interactions, but BNAH has only one amide carbonyl group at the C-3. As far as the DMPBIH and TMBIH donors are concerned, they have two electron-rich N's adjacent to the donor C in the 1,2-dihydroimidazoline ring, which is meanwhile fused with a π-electron-rich phenyl ring, largely increasing the π-π interactions. Also, they have the bulky Ph and CH_3 groups directly connected to the donor C, increasing the rigidity of the reaction sites. Due to the latter steric reason, the DMPBIH system would be more rigid than the TMBIH system. Therefore, it is expected that the rigidity would increase in order of systems of BNAH < HEH < TMBIH < DMPBIH.

The temperature dependence of the 1° H/D KIEs for the BNAH reaction in acetonitrile has been reported (by us).[37] In this work, the same for the other three systems in acetonitrile were carefully determined. The α-secondary (2°) KIEs at the 9-H/D position of the MA^+ were either reported previously (by us)[38] or determined in this work. They will be used to provide information for the relative rigidity at the reaction sites. The reactant complexes (CT complexes) involved in the reactions were determined spectroscopically. All possible productive reactant complex (PRC) geometries of each system were computed in an attempt to provide insight into the relationship between structure and DAD distributions in the TRSs. Evidence supporting the tunneling mechanisms will be presented. The steric effect on the 2° KIEs, the structure-rigidity relationship for the PRCs and TRSs, as well as the correlations of the temperature dependence of the 1° KIEs with the 2° KIEs and the DAD_{PRC} distributions, will be discussed. These will be compared with the similar correlations found in enzymes. The similarities and differences of the KIE behaviors in between solution and enzymes will be discussed. The important conclusion is that the more rigid the reaction centers, either caused by steric hindrance at the reaction site or by the electronic interactions from other parts of the structures, the weaker the temperature dependence of the 1° KIEs will be. The results appear to support the thermally activated DAD sampling concepts in the VA-AHT model and the corresponding explanations for enzymes.

Experimental

General procedures

Syntheses of the following compounds were previously reported from our group: 10-methylacridiniumion ($MA^+BF_4^-$), 9-deuterated-10-methylacridiniumion (MA^+-9-d), the Hantzsch ester (diethyl 1,4-dihydro-2,6-dimethyl-3,5-pyridinedicarboxylate, HEH), 1,2-dimehtyl-2-phenyl-1,2-dihydrobenzimidazoline (DMPBIH).[37,38] The 4,4'-dideuterated HEH (HEH-4,4'-d,d) was synthesized by reacting ethyl acetoacetate, ammonia with formaldehyde-d_2 following the literature procedure.[39] The DMPBIH-2-d was

prepared by reduction of the 1,3-dimethyl-2-phenyl-benzimidazolium iodide ($DMPBI^+I^-$) with $NaBD_4$ in anhydrous acetonitrile, following the same procedure as in literature.[40] The precursor salt for the latter, 1,3-dimethyl-2-phenyl-benzimidazolium iodide, was synthesized from the reaction of 2-phenylbenzimidazole with CH_3I in methanol in the presence of NaOH in a sealed tube at 120 °C for 10 hours, according to the method described in literature.[40] The syntheses of 1,2,3-trimethyl-benzimidazolium iodide ($TMBI^+I^-$) and 1,2,3-trimethylbenzimidazoline (TMBIH) used the same procedures for the preparation of the $DMPBI^+$ and DMPBIH, except that the commercially available 2-methylbenzimidazole was used. The TMBIH-2-d was prepared by reduction of the $TMBI^+I^-$ with $NaBD_4$ in methanol-d_4. The D content in all deuterated compounds are believed to be > 98% (by NMR). The ^1H NMRs for all of the hydride donors are included in *SI*.

The HPLC grade acetonitrile was carefully redistilled twice under nitrogen, with the presence of $KMnO_4/K_2CO_3$ (to remove the reducing impurity) and P_2O_5 (to remove water) in order, for kinetic measurements.

Kinetic procedures

All kinetics were determined in acetonitrile under pseudo-first-order conditions at certain temperatures. Measurements were conducted on an UV-Vis spectrophotometer with a thermostated cuvette connected to a rapid stopped-flow mixer (a Hi-Tech Scientific SFA-20 fast kinetic determination kit) or on a SF-61DX2 Hi-Tech KinetAsyst double-mixing stopped-flow instrument. The kinetics were determined to give the pseudo-first order rate constants (k^{pfo}) (R^2 are in the range of 0.9990 - 1.0000). The effect of substrate concentrations on k^{pfo} for each reaction was examined and the reactions follow the second-order rate law. This is consistent with the literature.[41-44] The KIEs were calculated using the second-order rate constants (k's). The measurements of the kinetics of the reactions of the two isotopologues for KIE derivation (= k_H/k_D) were done on the same day (back to back) using the same batch of distilled acetonitrile solvent (6 kinetic runs each) and were repeated on different days for the temperature range of 40 °C and/or 25 °C. We also often used different batches of substrates in the determination of the KIEs in order to test the effect of possible different impurity on the KIE measurements, and we did not find apparent differences. All of the kinetic data are summarized in Tables S2 to S5 in *SI*. Careful measurements were done and standard deviations are relatively small.

Specifically, kinetics were determined by following the decay of the MA^+ at 436 nm. The H-donors are in larger excess. The obtained $-\ln(A - A_\infty)$ *vs.* t data gave the k^{pfo}. Second-order rate constants ($k = k^{pfo}$/[H-donor]) were used to calculate the 1° KIEs.

$$1° \; KIE = \frac{k_H}{k_D} = \frac{k_H^{pfo}}{k_D^{pfo}} \times \frac{[Donor - d]}{[Donor - h]} \qquad (2)$$

In order to reduce the errors from the concentration terms so as to obtain the accurate KIE, the above concentration ratio was corrected by determining the absorbance (A) value of the H/D isotopic donor kinetic solutions at certain wavelength (at least three times each). Thus the KIE was derived according to eq (4) (assuming $\varepsilon_H = \varepsilon_D$),

$$1° \; KIE = \frac{k_H}{k_D} = \frac{k_H^{pfo}}{k_D^{pfo}} \times \frac{A_D}{A_H} \qquad (3)$$

For the measurement of α-2° KIE on MA^+, since the same donor was used, 2° KIE = k_H^{pfo}/k_D^{pfo}, in which the concentration terms as in eq (3) are cancelled.

The UV-Vis spectra of the CT complexes (reactant complexes (RCs)) were recorded upon mixing of the two reactants on the SF-61DX2 stopped-flow spectrophotometer.

Computational procedures

All structures were optimized using the M06-2X density functional that is parameterized specifically for thermochemical properties of main group elements and dispersion interactions.[45] Initial geometries of the TSs were first optimized using the Def2-SVP basis set[46], and the PRC structures were located from the intrinsic reaction coordinate analysis, in gas-phase. These structures were further refined by involving the acetonitrile solvent and using a larger Def2-TZVP basis set[46], the SMD solvation model[47], and the ultrafine DFT integral grid. These latter structures were used for the harmonic vibrational analysis to calculate their thermal corrections to the Gibbs free energies (E_{G_corr}) and the single point energies (E_{sp}). Gaussian 09 was used for all of the calculations.

Free energies (G) of the optimized structures are the sum of E_{G_corr} and E_{sp}. Since the zero-point vibrational energy (ZPVE) calculated using the harmonic model is overestimated, further treatments were needed to correct them to derive the E_{G_corr}. Scaling factor of 0.9708 was calculated to fit the theoretical ZPVEs from the harmonic model to the ZPVE15/10 database[48] for the purpose. Detailed procedure for calculating the scaling factor follows the method in literature.[48] The corrected ZPVEs were used to calculate the E_{G_corr}s.

To calculate the E_{sp}, we used the M06-2X density functional, the Aug-cc-pVTZ basis set,[49] and the SMD solvation model. The corresponding G (= $E_{G\_corr} + E_{sp}$) was then calculated.

The abundance (A_i) of each optimized conformation (i) for each reaction system was calculated according to the Boltzmann distribution of its energy (G_i) over the sum of such Boltzmann distributions for all of the conformations,

$$A_i = (e^{-\frac{G_i}{kT}}) / \sum_1^N e^{-\frac{G_i}{kT}} \qquad (4)$$

where N is the number of conformations, k is the Boltzmann constant, T is the temperature.

The weighted average DAD was calculated by summing up the fractional DADs of all of the conformations, each of which was obtained by multiplying the individual DAD_i with the corresponding abundance (A_i). The formula to calculate the weighted average DAD is as follows,

$$Weighted\ average\ DAD = \sum_1^N \mathrm{DAD_i}\, A_i \qquad (5)$$

Results

*From weak to strong temperature dependence of the 1° KIEs: Replication of the trend observed from wt-*enzymes *to mut-*enzymes

At the time when the temperature dependence of the 1° KIEs for the reaction of BNAH was measured, our rapid kinetic measurement instrument only allowed us to determine its fast kinetics at a temperature range from 5 to 30 °C.[37] We then also determined the same for the reaction with the iodide salt of the MA^+ and results are similar (not reported then). We found that the results are consistent with that of the reaction of its close analogue 1-(*p*-methylbenzyl)-1,4-dihydronicotinamide (MeBNAH) with MA^+I^- in the same solvent by Bruice and coworkers who had the ability to determine the rates for a much wider temperature range of 50 degrees.[50] All of these results are listed in Table 1 (columns 1 to 3),

Table 1. Temperature dependence of the 1° KIEs and activation parameters for the hydride transfer reactions in acetonitrile

Reaction System	BNAH/ $MA^+BF_4^-$ [a,b]	BNAH/ MA^+I^- [a]	CH_3BNAH/ MA^+I^- [c]	HEH/ $MA^+BF_4^-$ [a]	HEH/ $MA^+BF_4^-$ [d]	TMBIH/ $MA^+BF_4^-$ [d]	DMPBIH/ $MA^+BF_4^-$ [a]	DMPBIH/ $MA^+BF_4^-$ [d]
Column	1	2	3	4	5	6	7	8
Temp. range (°C)	4.5 ~ 29.5	4.5 ~ 29.5	-2.2 ~ 50.0	6.0 ~ 32.0	5.2 ~ 45.0	5.0 ~ 45.0	6.0 ~ 32.0	5.2 ~ 45.0
1° KIE range	4.93 ~ 3.93	4.87 ~ 3.74	6.42 ~ 4.00	5.61 ~ 4.81	5.41 ~ 4.42	2.84 ~ 2.52	3.79 ~ 3.56	3.70 ~ 3.37
ΔE_a (kcal/mol)	1.53 (0.15)	1.85 (0.31)	1.84 (0.25)	1.03 (0.07)	0.94 (0.12)	0.60 (0.10)	0.30 (0.14)	0.43 (0.15)
A_H/A_D	0.33 (0.11)	0.21 (0.11)	0.23 (0.69)	0.90 (0.11)	1.02 (0.23)	1.06 (0.25)	2.21 (0.54)	1.71 (0.45)
E_{aH} (kcal/mol)	5.42 (0.17)	4.78 (0.11)	8.22 (0.25)	5.27 (0.04)	6.30 (0.03)	7.60 (0.08)	6.38 (0.11)	7.80 (0.08)

[a] Using the Hi-Tech Scientific SFA-20 fast kinetic determination kit connected to a spectrophotometer (at the time when the instrument in footnote d was not available); [b] our published work[37]; [c] from reference;[50] [d] using the SF-61DX2 Hi-Tech KinetAsyst double-mixing stopped-flow instrument.

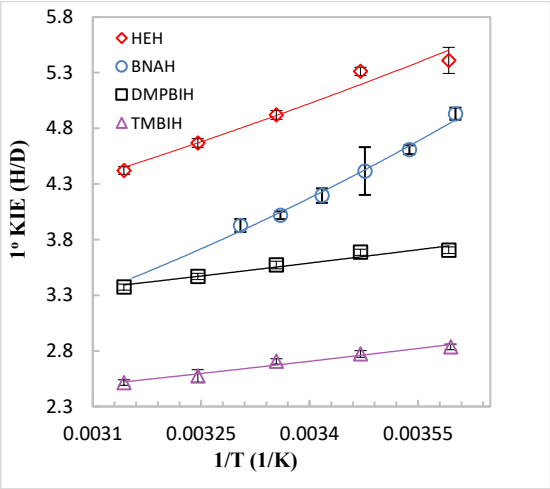

Figure 1. Arrhenius fit of the temperature dependence of the 1° KIEs of the hydride transfer reactions from various NADH models to $MA^+BF_4^-$ in acetonitrile over a 40 °C temperature range (data corresponding to columns 1, 5, 6 and 8 in Table 1). These are consistent with the fit to the data over the 25 °C temperature range (see Figure S1, and columns 1, 4, 7 in Table 1). The data for the BNAH reaction were from a temperature range of 25 °C and were reported from our group before.[37] They are consistent with the results for the reaction of CH_3BNAH over a temperature range of 50 °C (see texts and compare column 2 with column 3 in Table 1).

which includes the range of the 1° KIEs at temperatures applied and parameters characterizing their temperature dependency, which are, the isotopic activation energy differences ($\Delta E_a = E_{aD} - E_{aH}$) and the isotopic Arrhenius pre-exponential factor ratios (A_H/A_D). In the same table are also listed the results for the reactions of HEH (columns 4 and 5), TMBIH (column 6), DMPBIH (columns 7 and 8) using either the old instrument (for 25 degrees temperature range) or the new stopped-flow rapid kinetic measurement instrument (for 40 degrees temperature range), or both, determined in this work (see experiments and Table 1 footnotes for more information). Other activation parameters (enthalpy and entropy) along with the rate constants are listed in Tables S1 to S5 in Supporting Information (*SI*). The results from both instruments are consistent within the experimental errors. Note that the α-2° KIEs should be contained in the observed 1° KIEs for the reactions of BNAH and HEH as we used their 4,4'-h,h and 4,4'-d,d substrates (1° KIE_{obs} = 1° $KIE_{intrinsic}$ x 2° KIE). This will affect the A_H/A_D, but not the ΔE_a that we use for discussions in this paper (assuming that the small 2° KIE is temperature independent). The Arrhenius correlations for the four reactions are plotted in Figure 1 for a direct comparison. The ΔE_a decreases in order of the reactions of BNAH (1.53 kcal/mol) > HEH (0.99) > TMBIH (0.60) > DMPBIH (0.37) (the ΔE_a's for the reactions of HEH and DMPBIH are the average of the values measured from the 25°C and 40 °C temperature ranges.). To the best knowledge of the authors, the ΔE_a for the reaction of DMPBIH is the smallest (closest to 0) ever observed in the general bimolecular H-transfer reactions in solution.[37,50-53] It should be noted that all of the other NADH/NAD^+ model reactions previously reported showed the ΔE_a's much larger than 1.0 kcal/mol.[37,50,51]

The α-2° KIEs on MA^+: Effective ruler for the relative crowdedness/rigidity at the reaction centers

The 2° KIE can be an indicator of the crowdedness/rigidity around the reaction centers. The more sterically hindered it is around the 2° H, the more suppressed the 2° C-H/D bond vibrations are, the smaller the 2° KIE value will be. This is termed as a steric 2° KIE.[54,55] Therefore, it is expected that a more highly packed/rigid environment at the reaction centers would correspond with a smaller 2° KIE value.

The observed α-2° KIEs on MA^+ for its reactions with BNAH, HEH and DMPBIH in acetonitrile have been reported by us.[38] In this work, we determined the same with TMBIH. All of the 2° KIE_{obs}'s, from 1.00 to 1.02, are listed in Table 2 (Entry 1). Note that these 2° KIEs are similar (close to or larger than unity) to those at the α-C-H/D position of the analogous xanthylium ion with various hydride donors.[38,56] They are inflated relative to the semiclassically predicted values ($KIE_{classical}$'s), which are supposed to be inverse for an sp^2-to-sp^3 process. It has been commonly accepted that the inflated 2° KIE_{obs}'s in H-transfer reactions are caused by the 1° H tunneling mechanism, and the more extensive the tunneling, the more inflated the 2° KIE would be.[9,37,57-65] Therefore, use of these 2° KIE_{obs} values to evaluate and compare the stiffness of the α-2° C-H bond vibrations or rigidity of the corresponding reaction site, must consider the tunneling effects [65] as well as steric effects on the 2° KIEs. Tunneling effect inflates the 2° KIEs, but steric effect suppresses the inflations.

Table 2. α-2° KIE_{obs}'s at the 9-H/D position of MA^+ for its reactions with various hydride donors and free energy change ($\Delta G°$) of the reactions [a]

Entry	Hydride Donors			
	BNAH	HEH	TMBIH	DMPBIH
1	α-2° KIE_{obs} on hydride acceptor of MA^+ [b]			
	1.02 (0.01)	1.02 (0.01)	1.00 (0.01) [c]	1.00 (0.01)
2	$\Delta G°$ (kcal/mol) determined in acetonitrile [d]			
	-16.9	-11.3	~ or < -27.0 [e]	-27.0 [f]
3	Calculated gas-phase $\Delta G°$ (kcal/mol) [g]			
	-11.0	-6.7 [h]	-27.7	-28.0

[a] In acetonitrile, at 25 °C; [b] From ref.[38], otherwise indicated, numbers in parentheses are standard deviations; [c] This work; [d] From literature;[44,66] [e] See texts, ~ or < means slightly less negative than, according to $\Delta G°$ and Hammond's postulate; [f] The number of -23.6 kcal/mol in reference[38] should be corrected; [g] see *SI* for more details in calculations; [h] for HEH(Me), in which the ethyl in HEH is replaced by the methyl group for less computing time.

First, we need to know how much the inflation of the 2° KIEs is observed in each system (Δ(2°KIE) = KIE_{obs} - $KIE_{"classical"}$). The relative position of the assumed "classical TS" in the reaction coordinate is needed to evaluate the relative 2° $KIE_{"classical"}$. (Here the quoted "classical TS" is used to represent an assumed TS in which the 2° C-H bond's vibrations are not affected by the sterics from the donors so that its KIE only originates from the rehybridization of the reaction center in MA^+ during the reaction.) The empirical reasoning used for the latter purpose is that when the "classical TS" is reactant-like, the 2° $KIE_{"classical"}$ is closer to unity; and when the "classical TS" is product-like, it is closer to the corresponding equilibrium isotope effect.[67] The relative position of the "TSs" can be rationalized by comparing the free energy changes ($\Delta G°$'s) of the reactions. According to Hammond's postulate, the more negative the $\Delta G°$, the more reactant-like the "TS" with respect to the hybridizations of the reaction centers, the closer to unity the 2° KIE will be. Table 2 (entry 2) lists the distinctly different negative $\Delta G°$s for the reactions of BNAH, HEH, and DMPBIH, obtained from the experimentally determined hydride affinities of the corresponding oxidized forms of the donors including MA^+ in acetonitrile from literature.[44] There is no hydride affinity value reported for $TMBI^+$, but since it is most likely slightly less stable than $DMPBI^+$ due to the potentially greater stabilization effect on the cation by the phenyl group in the latter, the $\Delta G°$ for the reaction of TMBIH would be slightly less negative than that of DMPBIH. The above order in experimentally determined $\Delta G°$'s is consistent with our calculated relative gas-phase $\Delta G°$'s of the four reactions (entry 3 in Table 2, see *SI* for more information). Because all of these reactions are exergonic, the "TS's" are reactant-like, the inverse 2° $KIE_{"classical"}$'s should be closer to unity to different extents (as compared to the equilibrium isotope effect). Therefore, according to $\Delta G°$'s, the resemblance of the "TS's" to the reactants, and thus the theoretical 2° $KIE_{"classical"}$'s in relation to the closeness to unity, would be in order of the reactions of

DMPBIH (with most reactant-like "TS" and 2° $KIE_{"classical"}$ closest to unity) > TMBIH > BNAH > HEH.

Thus, the observed relative α-2° KIE inflations on MA^+ (Δ(2°KIE)) from the smallest to largest are in order of its reactions with

DMPBIH (observed smallest 2° KIE inflation) < TMBIH < BNAH < HEH.

The relative observed 2° KIE inflations are described in Scheme 2 (with black ↑ arrows).

In order to evaluate the steric suppression effect, if any, on the 2° KIE inflations, the relative extent of tunneling contribution to the inflation needs to be known. From the observed temperature dependency of the 1° KIEs (Table 1), we know that the tunneling extents of the systems are different. The traditional Bell model of H-tunneling suggests that the ΔE_a smaller than about 1.0 kcal/mol corresponds to large to extensive extent of tunneling (deep tunneling), and that larger than about 1.2 kcal/mol corresponds to small to moderate extent of tunneling (shallow tunneling) (one could also use the isotopic Arrhenius pre-exponential ratios (A_H/A_D) for such analysis).[68,69] Note that the ΔE_a from 1.0 ~ 1.2 kcal/mol is the theoretical semiclassical range. Contemporary models suggest that tunneling also happens when ΔE_a is within this range, and the smaller the ΔE_a, the more extensive the tunneling is.[70] (Indeed, some workers have uncovered that the Bell model itself overlooks a fact that the tunneling within the Bell model could also happen when ΔE_a = 1.0 ~ 1.2 kcal/mol (or A_H/A_D ~ 1) at certain temperature range.[69]) Therefore, according to ΔE_a's (Table 1), the

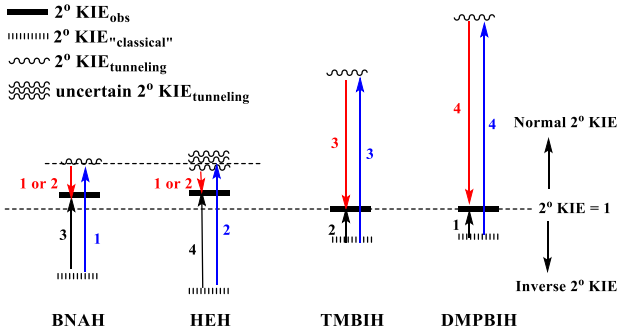

Scheme 2. Schematic description of the relative observed inflations of the α-2° KIEs on MA^+ for its reactions with different donors (KIE_{obs} - $KIE_{"classical"}$) (black ↑ arrows), the supposed relative 2° KIE inflations due to tunneling only ($KIE_{tunneling}$ - $KIE_{"classical"}$) (blue ↑ arrows), and the relative degree of suppression of the 2° KIE inflations due to the crowding effects at the reaction sites ($KIE_{tunneling}$ - KIE_{obs}) (red ↓ arrows) for the reactions of four hydride donors with MA^+. The relative $KIE_{"classical"}$'s are evaluated from the relative $\Delta G°$s of the reactions, thus only reflecting the hybridization change of the reaction center of MA^+ during activation (assuming no steric effect involved). The relative $KIE_{tunneling}$'s are evaluated from the relative ΔE_a's. Numbers from 4 to 1 represent the degrees of inflations or suppressions, with 4 being the largest. Since the 2° $KIE_{"classical"}$ with HEH is more inverse than with BANH, and the 2° KIE inflation due to tunneling is more with HEH than with BNAH, it is not possible to quantitatively compare the 2° $KIE_{tunneling}$ for the two. So the position of the squiggly line representing $KIE_{tunneling}$ for the HEH reaction is uncertain relative to that of the BNAH reaction. Also there is a possibility that the steric effects on the 2° KIEs of the systems of BNAH and HEH are little so that the 2° $KIE_{tunneling}$'s are extremely close to the 2° KIE_{obs}'s (see texts).

tunneling extent would decrease in order of the reactions of

DMPBIH (highest extent of tunneling) > TMBIH > HEH > BNAH.

Since a higher tunneling probability would give rise to a larger 2° KIE inflation, the order of the supposed 2° KIE inflations due to tunneling only, decreases in order of the reactions of

DMPBIH (supposed most inflated 2° KIE due to tunneling) > TMBIH > HEH > BNAH (see blue ↑ arrows in Scheme 2).

The above supposed 2° KIE inflation order is, however, almost completely opposite to the observed order of inflations (blue arrows versus black arrows in Scheme 2), suggesting there is a steric effect from H-donors that suppresses the 2° KIE inflations. For example, the inflation due to tunneling would have been the largest for the reaction of DMPBIH (longest blue arrow), but the observed inflation is the smallest (shortest black arrow). While the reactions of DMPBIH and TMBIH have more suppressions of the 2° KIE inflations than those of HEH and BNAH, the relative 2° KIE suppression for the last two reactions are not distinguishable due to the uncertain relative 2° KIEs caused by tunneling between the two (see Scheme 2 for details). Therefore, the relative suppression of the 2° KIE inflations of the four systems decreases in order of the reaction of

DMPBIH (most suppressed 2° KIE inflation) > TMBIH > HEH (> or < ?) BNAH (see red ↓ arrows in Scheme 2).

Then, the crowding effects at the reaction center of the systems, from the 2° KIE evidences, decrease in order of the reaction of

DMPBIH (most crowded at the reaction center) > TMBIH > HEH (> or < ?) BNAH.

The crowdedness at the reaction centers of the reactions of BNAH and HEH could not be distinguished using the 2° KIEs. Meanwhile there is possibly little steric effect on the 2° C-H vibrations in both of the systems (As such, the observed KIE inflations are only resulted from the tunneling effect.). This may stand as these two donors do not have apparent steric factors directly attached to the reaction centers, different from DMPBIH and TMBIH in which the former has a Ph group and the latter a less bulky Me group at the donor C. But the following DAD_{PRC} analysis of the systems clearly suggests that the HEH/MA^+ is most likely more closely associated than the BNAH/MA^+ at their TRSs, via electronic interactions.

The productive reactant complex (PRC) structures, population of DAD_{PRC}'s: Further evidence to help finalize the rigidity order of the reaction centers

It is well known that hydride transfer reactions of NADH/NAD^+ analogues take place in a productive electron donor(Don-H)-acceptor(Acc) complex (or CT complex, here called productive reactant complex (PRC)) (eq 6).[71,72] Acquiring the PRC structures would help understand the structures of the TRSs. We attempted to use the stopped-flow UV-Vis spectroscopic technique to capture them. The CT absorption bands of all systems were obtained upon mixing of the reactants under certain concentration conditions and their decays with time were recorded (λ_{max} from 520nm to 600nm, see Figure S1 in *SI*). Since the observed absorptions are supposed to be due to both the non-productive and productive complexes (eq 2), there is no way to identify the absorptions for the PRCs only.

$$\text{Don-H + Acc} \underset{\text{fast}}{\rightleftharpoons} \text{Don-H/Acc (PRCs)} \xrightarrow{k} \text{Products} \quad (6)$$

$$\text{Don-H/Acc (PRCs)} \overset{\text{fast}}{\searrow} \text{Non-productive RCs} \overset{\text{fast}}{\nearrow} \text{Don-H/Acc (PRCs)}$$

Ideally, the equilibrium constant (K_{PRC}) would be determined so as to provide insight into the relative tightness/rigidity of the PRCs.[73] But this is not the case here as it is impossible to isolate the K_{PRC} from the observed K_{obs} value. Nonetheless, we attempted to determine the K_{obs}'s by following the change of absorptions with concentrations, but failed as the reactant concentration ranges that are able to produce measurable absorptions were limited and the complexes are unstable.

We then turned to seek help from computations to acquire the structures of the PRCs. The classical TS structures were first computed, and then the corresponding PRC structures were located from the intrinsic reaction coordinates derived from the respective TSs. (Note that literature[22] uses the similar strategy to evaluate the TRS rigidities and calls the PRCs as reactive complexes.) All calculations involve acetonitrile as the reaction medium. The resultant PRCs are assumed to be those that can be directly activated to the TRSs. This assumption may stand as the classical TS and TRS would be reached along the same potential energy surface except that the TRS arrives earlier. Note that we used the dimethyl ester group (in HEH(Me)) to replace the diethyl ester group in HEH for less computing time. For all of the systems, more than one TS/PRC were found. The systems of BNAH, HEH(Me), TMBIH, and DMPBIH have 21, 8, 2, and 3 distinctive PRCs and hence the same number of TRSs, respectively (the mirror image structures are not counted). The Gibbs free energies (G's) of the PRC structures for each system were calculated in order to calculate the populations of the PRCs (percentage of each PRC among the whole). All of the PRC structures along with their DAD_{PRC}'s and G's can be found in Tables S7 to S10 in *SI*. Figure 2 only presents the most populated PRC geometries. Figure 3 shows the abundance of the PRCs as a function of DADs for all of the four systems (Data come from the Tables S7 to S10 in *SI*). Table 3 lists the range of the DAD_{PRC}'s (shortest to longest), the weighted average DAD_{PRC}, the average DAD_{PRC}, and the DAD_{PRC} of the most populated PRC structure, in each system.

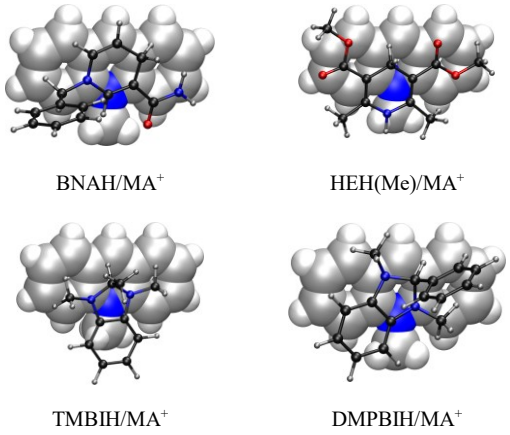

Figure 2. The geometries of the most populated PRCs (with the lowest free energy (G)) of the hydride transfer reactions from different hydride donors to MA^+ in acetonitrile at 25 °C. The back space-filling structure represents MA^+, the front ball-stick structures represent different donors. The blue and red atoms represent N and O, respectively. See Tables S7-S10 for all of the geometries.

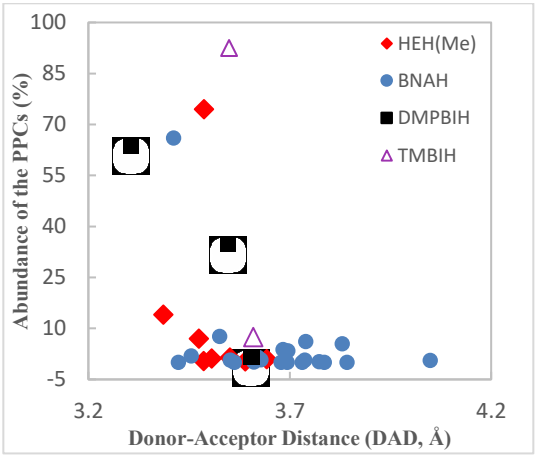

Figure 3. The donor-acceptor distance (DAD) distributions of the PRCs of the hydride transfer reactions from different donors to MA^+ in acetonitrile at 25 °C. All of the geometries can be found in Tables S7 to S10 in *SI*, respectively.

Table 3. Various types of DAD_{PRC}'s in the PRC complexes of the reactions of four hydride donors with MA^+ [a]

	Hydride Donors			
DAD_{PRC} (Å)	BNAH	HEH(Me)	TMBIH	DMPBIH
(# of PRCs)	(21)	(8)	(2)	(3)
Range	3.41~4.05	3.39~3.64	3.55~3.61	3.31~3.60
Weighted-average [b]	3.50	3.48	3.56	3.39
Average	3.67	3.51	3.58	3.49
In most populated PRCs [b]	3.41	3.49	3.55	3.31

[a] In acetonitrile at 25 C; [b] According to the percent populations of the PRCs.

In enzyme catalysis investigations, the ability of sampling multiple distances and conformational states is an indicator of enzyme flexibility. Here in our cases, temporarily putting the reaction of TMBIH aside, the reaction of BNAH has the largest number of PRCs (21) that cover the widest range of DAD_{PRC}'s from 3.41 to 4.05 Å, whereas those of the HEH(Me) and DMPBIH have 8 and 3 PRCs with DAD_{PRC}'s ranging from 3.39 to 3.64 Å and from 3.31 to 3.60 Å, respectively (Figure 3). The latter two DAD ranges are comparable, but the DMPBIH reaction has the smallest number of PRCs (and shortest DAD_{PRC}'s). These suggest that overall, the broadness of the DAD_{TRS} distributions in the TRSs would decrease from BNAH to HEH to DMPBIH, and thus the rigidity of the TRSs would be expected to increase from BNAH to HEH to DMPBIH. The highest rigidity of the DMPBIH system concluded from this analysis is consistent with the observed most suppressed 2° KIE inflation in the same system. In the 2° KIE analysis, we were not able to differentiate the rigidity order for the reactions of BNAH and HEH. Here the DAD_{PRC} distribution comparison clearly suggests that the reaction of HEH would have a more tightly associated TRS than does the reaction of BNAH. As far as the reaction of TMBIH is concerned, it has only 2 PRCs with DAD_{PRC}'s differing by only 0.06 Å. Therefore, it likely has very narrowly distributed DAD_{TRS}'s to suggest a highly rigid TRS. Combining with the rigidity order derived from the 2° KIEs above, a rigidity order of the four systems with regard to the extent of the vibrations of the two reaction centers can be given as follows (in terms of reactions with MA^+):

DMPBIH (most rigid) > TMBIH > HEH > BNAH (least rigid).

This rigidity order is within our expectation (See Introduction). It should be noted that the similar strategies have been used to compare the compactness/rigidity of the active sites of *wt*-enzymes versus *mut*-enzymes. For example, for the hydride transfer from NADH to morphinone mediated by the morphinone reductase (MR), the α-2° KIE on NADH was found to increase with increasing DAD_{PRC}'s from wild-type (short) to mutated (long) enzymes.[32] It was also observed that in two methyltransferases, Glycine *N*-Methyltransferase and Catechol *O*-methyltransferase, the 2° KIEs at the transferring CH_3/CT_3 (T-tritium) groups increase from *wt*-enzymes (short DAD_{TRS}) to *mut*-enzymes (long DAD_{TRS}).[74,75]

The weighted average DAD_{PRC}'s decrease in order of the reactions of TMBIH (3.56 Å) > BNAH (3.50 Å) > HEH(Me) (3.48 Å) > DMPBIH (3.39 Å). The order of the average DAD_{PRC}'s is, BNAH (3.67 Å) > TMBIH (3.58 Å) > HEH(Me) (3.51 Å) > DMPBIH (3.49 Å). Interestingly, the trends seem to suggest that the more rigid system prefers to have a shorter (weighted) average DAD in these systems (with TMBIH as an outlier).

Discussion

H-tunneling Models and Structure–ΔE_a Relationship

Traditionally, H-tunneling has been described with the semiclassical TS theory including correction terms that assumes a static energy barrier. This is called the Bell tunneling model.[68] 1° KIE is defined on the basis of the isotopic zero-point energy difference at the reactant state versus TS. Tunneling is proposed when the size of the 1° H/D KIEs and their temperature dependence are outside of the semiclassical limits; which are (i) the KIE is smaller than 9 (at 20 °C), (ii) the ΔE_a is within the range from 1.0 to 1.2 kcal/mol, and (iii) the A_H/A_D falls in the range from 0.7 to 1.4.[68,76,77] This model, however, does not involve heavy atom motions, and does not predict any form of the relationship between structure/DAD and ΔE_a.

The VA-AHT model that could include the nonadiabatic H-tunneling models and the extension of the TS theory (TST extension model)[15], the latter of which was proposed to be applicable to the adiabatic hydride tunneling reactions as well, can link the ΔE_a to the structurally determined DAD_{TRS}'s/rigidities. Within these full-tunneling theories, there are two activation processes. One is the heavy atom reorganization coordinate — the thermal energy is required for the donor and acceptor to reach an activated TRS in which the double potential wells of the reactant $[Don\text{-}H]^{\neq}$ and product $[Acc\text{-}H]^{\neq}$ are degenerate. This can occur at different DAD_{TRS}'s. The other activation process concerns sampling of the DAD_{TRS}'s, *i.e.*, the gating coordinate — thermal energy is needed to activate the molecular skeleton vibrations, i.e., the heavy atom motions, so as to sample the DAD_{TRS}'s for efficient H-wave function overlap, *i.e.*, H-tunneling. This implicates a vibrational TRS with fluctuating DADs, *i.e.*, a variational energy barrier. Only the latter gating coordinate is 1° isotope sensitive, determining the 1° KIE, which here is defined to be a ratio of the overall wave function overlap of H over that of D at all possible DAD_{TRS}'s. Therefore, the temperature dependence of the 1° KIEs is ascribed to the temperature dependence of the DAD_{TRS} distributions, i.e., the rigidity of the reaction centers. The broader the DAD_{TRS} distributions, the larger the ΔE_a is.

It should be noted that another popular model of H-tunneling, EA-VTST/MT, contains all the parameters in the VA-AHT model.[34] Its beauty is the rate calculations including all possible tunneling pathways through complex computations. That model, however, does not provide a straight-forward relationship between ΔE_a and DADs. Nonetheless, calculations of the H-transfer processes in thymidylate synthase following this model combined with the Grote-Hynes theory showed the same tunneling TS geometries (same DADs) at all temperatures applied, suggesting that the observed $\Delta E_a = 0$ does correspond with a temperature independence of the DAD_{TRS}'s.[28] On the other hand, however, the model was applied to simulate the temperature independence of the 1° KIEs for the dihydrofolate reductase from *E. coli*. (*ec*DHFR), and it was found that the 1° KIE behavior was caused by different positions of the tunneling TS and different effective potential barriers, which play opposite effects on their temperature dependency, producing temperature independent 1° KIEs.[27]

Preliminary Analysis of the observed ΔE_a's within the Traditional Bell Model of H-Tunneling

As mentioned earlier, the past few studies of the reactions of the $NADH/NAD^+$ analogues show larger ΔE_a (> 1.2 kcal/mol) and smaller A_H/A_D (<< 1).[37,50,51] These together with our previously published unusual 2° KIEs for some of those systems suggest that this type of bimolecular hydride transfer reactions take place by a non-classical H-tunneling mechanism.[37,38]

From Table 1 and Figure 1, the ΔE_a (or A_H/A_D) for the reactions of MA^+ with BNAH, HEH, TMBIH and DMPBIH in acetonitrile are 1.53 kcal/mol (or 0.33 for A_H/A_D), 0.99 kcal/mol (0.95), 0.60 kcal/mol (1.06), and 0.37 kcal/mol (1.96), respectively. Within the Bell model, the results suggest that the BNAH reaction takes place by a moderate H-tunneling mechanism, the HEH reaction takes place by a classical mechanism, and the TMBIH and DMPBIH reactions use a nearly full-tunneling mechanism for both H- and D-transfer processes. Here, however, there are two points that are contradictive to the Bell explanation. First, the DMPBIH reaction has a very small ΔE_a (close to zero), which should result at very low temperatures where the E_a is very small close to zero for both H- and D-transfers.[69] But all of the rates in this work were determined at around room temperature and its E_a is even slightly larger than those of the reactions of HEH and BNAH that would

have either no tunneling or moderate tunneling according to their ΔE_a's or A_H/A_D's (Table 1). Second, the KIEs of the three systems are small (< 6), within the semiclassical limit. Our results cannot be explained by the Bell model.

Correlation of the ΔE_a's to the rigidities of the reaction centers

The correlation of the ΔE_a's with the ground state DAD_{PRC}'s as well as 2° KIEs to support the DAD_{TRS} sampling gating coordinate in the VA-AHT model has been carried out in *wt*-enzyme/*mut*-enzyme studies. Scrutton and coworkers correlated the ΔE_a with the DAD_{PRC}'s determined for the hydride transfer from NADH to flavin mononucleotide (FMN) in the morphinone reductase (MR), and found that ΔE_a increases as DAD_{PRC} increases from *wt*-enzyme to *mut*-enzymes (They used the nonreactive $NADH_4$ with a tetrahydropyridine ring to replace the NADH in the DAD_{PRC} measurements).[32] They also found that the ΔE_a increases with increasing the α-2° KIE values on NADH. Kohen and coworkers computed the DAD_{PRC} fluctuating ranges of all possible enzyme–substrate complexes for the *ec*DHFR and its *mut*-enzyme and found that the ΔE_a is correlated with the DAD_{PRC} distributions very well; that is, the narrower the DAD_{PRC} distributions the smaller the ΔE_a.[22] Klinman and coworkers determined the structure of the enzyme-substrate complex between a manganese substituted soybean lipoxygenase (SLO(Mn)) and the linoleic acid (LA) substrate.[78] They found that there are two conformations of the ground state complexes. The SLO(Mn)-LA complex has a shorter DAD_{PRC} of 3.1 Å and a noncatalytic longer DAD_{PRC} of 3.9 Å. When an SLO(Mn) *mut*-enzymes I553G was used, the conformation of the shorter DAD_{PRC} disappeared. The two conformers were also confirmed by the QM/MM and DFT computations by Hammes-Schiffer's group[26] and Chapman's group[25], respectively. Importantly, these are consistent with the observed ΔE_a of 0.9 kcal/mol (small) in SLO and 5.3 kcal/mol (large) in its *mut*-enzyme SLO I533G, respectively.

In this work, a correlation between ΔE_a and rigidity of our systems (from both the 2° KIE and DAD_{PRC} distribution results) in solution shows the same trend as in *wt*-enzymes (with rigid TRS) versus *mut*-enzymes (with loose TRS), which is, the more rigid the system/TRS the smaller the ΔE_a. The rigidity order from most to least rigid system is: DMPBIH > TMBIH > HEH > BNAH, whereas the ΔE_a order from largest to smallest values is opposite: BNAH > HEH > TMBIH > DMPBIH. Our results are consistent with the observed trend of the ΔE_a's in *wt*-enzymes versus *mut*-enzymes and appear to support the explanations therein using the concepts of thermal motions and DADs in the VA-AHT model.

Comparison of the effects of reactant versus protein structures on ΔE_a's

Since all of the hydride donors in this work are NAD(P)H mimics, and the hydride acceptor MA^+ can be a mimic of the protonated dihydrofolate ($DHFH^+$) (both contain $C=N^+$- group that is directly or indirectly reduced by a hydride ion.), our reactions can be models of the hydride transfer reactions from NADPH to $DHFH^+$ catalyzed by DHFR enzymes.[79] The temperature dependence of the 1° KIEs for the wild-type *ec*DHFR and *mut*-enzymes have been determined and used to extensively discuss the protein coupled motions.[22,80] In this enzyme, the amino acid residue I14 that is situated near the nicotinamide ring of NADPH and involved in the network of protein motions regulates the DAD_{TRS} and its distributions.[22] When the size of the amino acid decreases from mutation, the DAD_{TRS} and ΔE_a were found to increase. While the ΔE_a of the model reactions in solution ranges from 0.37 (with DMPBIH) to 1.53 kcal/mol (BNAH) in this work, the ΔE_a's of the *ec*DHFR reactions have a much broader range from about 0 (for the *wt*-enzyme) to 3.31 kcal/mol (for a *mut*-enzyme I14G). Here we claim that we have replicated the trend (weak to strong) of the temperature dependence of 1° KIEs of enzymes in solution, but we have not shown the trend as broad as from *wt*-enzymes to *mut*-enzymes. Whether the bimolecular model reactions are able to show the absolute temperature independence of the 1° KIEs that was frequently observed in the wild-type enzymes, and how strong the temperature dependence of the 1° KIEs one can find through changing the structures, are still in question. We are not sure if we can eventually find a bimolecular model system that produces a $\Delta E_a = 0$, but we may be able to broaden the upper limit by modifying the structures near or remote from the reaction center and allowing them to interact in a way that impairs the constructive vibrations near the reaction centers.

Conclusions

In this paper, we proposed to study the structure–ΔE_a relationship for H-transfer reactions in solution. This study has not been systematically done so far but has been advocated to study by the enzymologists. The protein structure–ΔE_a relationship for the reactions in *wt*-enzymes and *mut*-enzymes have been studied in the past 20 years. The frequently observed ΔE_a increasing with change from *wt*-enzymes to *mut*-enzymes has promoted enzymologists to establish a relationship between ΔE_a and DADs in the TRSs, which has been included in the VA-AHT model (also called the Marcus-like model or the extension of TST). The nonadiabatic form of the models was initially developed on the basis of a previous theoretical model put forth by Kuznetsov and Ullstrup.[12,81] These models predict that, the more narrowly distributed the DAD_{TRS}'s, the smaller is the ΔE_a. This relationship has been used by some enzymologists to relate the magnitude of ΔE_a with the enzyme thermal motions/dynamics that sample the short DADs for H-tunneling to take place. But the models have not been fully accepted by the scientific field. The overall purpose of our study is to find a more general relationship between structure and ΔE_a for simpler H-transfer reactions in solution in an attempt to provide insight into these models and the relevant arguments. This will make the theoreticians relatively easier to fit the results by treating smaller number of atoms to different models to find whether there is a dynamic effect on the C-H activations in solution. This study opens a new physical organic chemistry research direction that investigates how structure affects the temperature dependence of the 1° KIEs in H-transfer reactions.

We designed hydride transfer reactions from four distinctively different NADH model structures (BNAH, HEH, TMBIH and DMPBIH) to the same hydride acceptor MA^+ to study the structure–ΔE_a relationship in acetonitrile. The ΔE_a's (ranging from 0.37 ~ 1.53 kcal/mol) and the α-2° KIEs on MA^+ were determined. The DAD_{PRC} distributions were computed. The more suppressed 2° KIEs and the more narrowly distributed and/or the shorter DAD_{PRC}'s would correspond to a rigid TRS. The correlation between rigidities and ΔE_a's shows the same trend as observed in *wt*-enzymes versus *mut*-enzymes; that is, the more narrowly distributed and/or the shorter the DADs, the smaller is the ΔE_a. Our results appear to support the thermal motions and DAD concepts in the VA-AHT model and corresponding explanations in enzymes. The trend, however, does not cover as broad ΔE_a/DAD ranges as observed in *wt*-enzymes and *mut*-enzymes , which will be a future target to study. We do not yet know at the moment whether the $\Delta E_a = 0$ can be found in a bimolecular H-transfer reaction in solution, which might be unique to the *wt*-enzymes that have been evolved over the millions of years, but we believe that we can broaden the upper limit by modifying the structure(s) near or remote from the reaction center that lengthen the DADs and disturb the constructive

vibrations. Furthermore, we would like to see whether our results will be able to be fitted into other models of H-tunneling by other research groups to discuss/argue about the complex role of heavy atom motions in the C-H bond activation chemistry. Further study of the structure–ΔE_a relationship for various hydride transfer reactions in solution is in progress in this laboratory. This includes the solvent effects on the TRS structures and thus the ΔE_a's. On the other hand, it should be noted that here we are using the 1° KIEs in solution to testing the role of fast motions in enzyme catalysis, but one must be aware that certain slow motions also influence catalysis, for example, through sampling the conformational substrates that promote reaching a TS/TRS.[82]

Finally, it should be noted that studies of temperature dependence of the 1° KIEs have been extensively reported for proton transfer reactions in solution, but they were not designed to investigate the concepts of DADs and heavy atom motions. Almost all of them showed large ΔE_a's, as large as 4.6 kcal/mol.[52,83] They were thus discussed on the basis of the Bell model of H-tunneling. A possible explanation is that the proton transfer systems usually do not have strong electronic interactions between substrates as in hydride transfer reactions. But it is our belief that the weak temperature dependence of the 1° KIEs for proton transfer reactions would be able to be found if careful designs of rigid systems are made.

ASSOCIATED CONTENT

Supporting Information

Detailed kinetic data, CT absorption bands, atom coordinates and total energies of the structures, calculation of the gas-phase ΔG°'s, synthesis of TMBIH and deuterated analogue, ^{1}H NMRs. This material is available free of charge via the Internet at http://pubs.acs.org.

AUTHOR INFORMATION

Corresponding Author

* yulu@siue.edu

Notes

The authors declare no competing financial interests.

† The two authors contribute the same amount of work.

ACKNOWLEDGMENT

Acknowledgment is made to the donors of the National Science Foundation (NSF# 1800194) and the XSEDE startup allocation for access to the facilities of the Pittsburg supercomputing center (CTS170029) for supporting of this research.

REFERENCES

(1) Antoniou, D.; Schwartz, S. D.: Large kinetic isotope effect in enzymatic proton transfer and the role of substrate oscillations. *Proc. Natl. Acad. Sci. USA* **1997**, *94*, 12360-12365.

(2) Kohen, A.; Cannio, R.; Bartolucci, S.; Klinman, J. P.: Enzyme dynamics and hydrogen tunnelling in a thermophilic alcohol dehydrogenase. *Nature* **1999**, *399*, 496-499.

(3) Benkovic, S. J.; Hammes-Schiffer, S.: A perspective on enzyme catalysis. *Science* **2003**, *301*, 1196-1202.

(4) Hay, S.; Sutcliffe, M. J.; Scrutton, N. S.: Promoting motions in enzyme catalysis probed by pressure studies of kinetic isotope effects. *Proc. Natl. Acad. Sci. U.S.A.* **2007**, *104*, 507-512.

(5) Agarwal, P. K.; Billeter, S. R.; Rajagopalan, P. T. R.; Benkovic, S. J.; Hammes-Schiffer, S.: Network of coupled promoting motions in enzyme catalysis. *Proc. Natl. Acad. Sci. USA* **2002**, *99*, 2794–2799.

(6) Hay, S.; Scruton, N. S.: Good vibrations in enzyme-catalysed reactions. *Nature Chemistry* **2012**, *4*, 161-168.

(7) Wang, Z.; Singh, P. N.; Czekster, M. C.; Kohen, A. S., V.L.: Protein Mass-Modulated Effects in the Catalytic Mechanism of Dihydrofolate Reductase: Beyond Promoting Vibrations. *J. Am. Chem. Soc.* **2014**, *136*, 8333-8341.

(8) Klinman, J. P.; Kohen, A.: Hydrogen Tunneling Links Protein Dynamics to Enzyme Catalysis. *Annu. Rev. Biochem.* **2013**, *82*, 471–496.

(9) Nagel, Z. D.; Klinman, J. P.: Update 1 of: Tunneling and dynamics in enzymatic hydride transfer. *Chem. Rev.* **2010**, *110*, PR41–PR67.

(10) Hay, S.; Sutcliffe, M. J.; Scruton, N. S.: Probing Coupled Motions in Enzymatic Hyfrogen Tunneling Reactions: Beyond Temperature-Dependence Studies of Kinetic Isotope Effects. In *Quantum Tunnelling in Enzyme-Catalyzed Reactions*; Scrutton, N. S., Allemann, R. K., Eds.; RSC Publishing, 2009; pp 199-218.

(11) Sen, A.; Kohen, A.: Quantum Tunnelling in Enzyme Catalyzed Reactions. In *Quantum Effects in Enzyme Kinetics*; Allemann, R., Scrutton, N., Eds.; Royal Society of Chemistry: London, UK, 2009; pp 164-181.

(12) Knapp, M. J.; Rickert, K.; Klinman, J. P.: Temperature-dependent isotope effects in soybean lipoxygenase-1: Correlating hydrogen tunneling with protein dynamics. *J. Am. Chem. Soc.* **2002**, *124*, 3865-3874.

(13) Hammes-Schiffer, S.: Hydrogen tunneling and protein motion in enzyme reactions. *Acc. Chem. Res.* **2006**, *39*, 93-100.

(14) Schwartz, S. D.: Vibrationally enhanced tunneling and kinetic isotope effects in enzymatic reactions. In *Isotope effects in chemistry and biology*; Kohen, A., Limbach, H. H., Eds.; Taylor & Francis, CRC Press: Boca Raton, FL, 2006; Vol. Ch. 19; pp 475-498.

(15) Kohen, A.: Role of Dynamics in Enzyme Catalysis: Substantial vs. Semantic Controversies. *Acc. Chem. Res.* **2015**, *48*, 466-473.

(16) Basran, J.; Sutcliffe, M. J.; Scrutton, N. S.: Enzymatic H-Transfer Requires Vibration-Driven Extreme Tunneling. *Biochemistry* **1999**, *38*, 3218-3222.

(17) Harris, R. J., Meskys, R., Sutcliffe, M. J., Scrutton, N. S.: Kinetic Studies of the Mechanism of Carbon−Hydrogen Bond Breakage by the Heterotetrameric Sarcosine Oxidase of Arthrobacter sp. 1-IN. *Biochemistry* **2000** *39*, 1189-1198.

(18) Basran, J.; Sutcliffe, M. J.; Scrutton, N. S.: Deuterium Isotope Effects during Carbon–Hydrogen Bond Cleavage by Trimethylamine Dehydrogenase: Implications for mechanism and vibrationally assisted hydrogen tunneling in wild-type and mutant enzymes. *J. Biol. Chem.* **2001**, *276*, 24581-24587.

(19) Knapp, M. J.; Klinman, J. P.: Environmentally coupled hydrogen tunneling. Linking catalysis to dynamics. *Eur. J. Biochem.* **2002**, *269*, 3113–3121.

(20) Sikorski, R. S.; Wang, L.; Markham, K. A.; Rajagopalan, P. T. R.; Benkovic, S. J.; Kohen, A.: Tunneling and coupled motion in the *E. coli* dihydrofolate reductase catalysis. *J. Am. Chem. Soc.* **2004**, *126*, 4778-4779.

(21) Wang, Z.; Kohen, A.: Thymidylate synthase catalyzed H-transfers: Two chapters in one tale. *J. Am. Chem. Soc.* **2010**, *132*, 9820–9825.

(22) Stojkoviç, V., Perissinotti, L., Willmer, D., Benkovic, S., and Kohen, A.: Effects of the donor acceptor distance and dynamics on hydride tunneling in the dihydrofolate reductase catalyzed reaction. *J. Am. Chem. Soc.* **2012**, *134*, 1738-1745.

(23) Hu, S.; Soudackov, A. V.; Hammes-Schiffer, S.; Klinman, J. P.: Enhanced Rigidification within a Double Mutant of Soybean Lipoxygenase Provides Experimental Support for Vibronically Nonadiabatic Proton-Coupled Electron Transfer Models. *ACS Catal.* **2017**, *7*, 3569−3574.

(24) Hatcher, E.; Soudackov, A. V.; Hammes-Schiffer, S.: Proton-coupled electron transfer in soybean lipoxygenase. *J. Am. Chem. Soc.* **2004**, *126*, 5763-5775.

(25) Salna, B.; Benabbas, A.; Russo, D.; Champion, P. M.: Tunneling kinetics and nonadiabatic proton-coupled electron transfer in proteins: The effect of electric fields and anharmonic donor-acceptor interactions. *J. Phys. Chem. B* **2017**, *121*, 6869−6881.

(26) Li, P.; Soudackov, A. V.; Hammes-Schiffer, S.: Fundamental insights into proton-coupled electron transfer in soybean lipoxygenase from quantum mechanical/molecular mechanics free energy simulations. *J. Am. Chem. Soc.* **2018**, *140*, 3068-3076.

(27) Pu, J.; Ma, S.; Gao, J.; Truhlar, D. G.: Small temperature dependence of the kinetic isotope effect for the hydride transfer reaction catalyzed by

Escherichia coli dihydrofolate reductase. *J. Phys. Chem. B* **2005**, *109*, 8551−8556.
(28) Kanaan, N.; Ferrer, S.; Martí, S.; Garcia-Viloca, M.; Kohen, A.; Moliner, V.: Temperature Dependence of the Kinetic Isotope Effects in Thymidylate Synthase. A Theoretical Study. *J. Am. Chem. Soc.* **2011**, *133*, 6692–6702.
(29) Delgado, M. G., S.; Longbotham, J. E.; Scrutton, N. S.; Hay, S.; Moliner, V.; Tuñón, I.: Convergence of Theory and Experiment on the Role of Preorganization, Quantum Tunneling, and Enzyme Motions into Flavoenzyme-Catalyzed Hydride Transfer. *ACS Catal.* **2017**, *7*, 3190–3198.
(30) Liu, H.; Warshel, A.: Origin of the Temperature Dependence of Isotope Effects in Enzymatic Reactions: The Case of Dihydrofolate Reductase. *J. Phys. Chem. B* **2007**, *111*, 7852–7861.
(31) Kamerlin, S. C. L.; Warshel, A.: An analysis of all the relevant facts and arguments indicates that enzyme catalysis does not involve large contributions from nuclear tunneling. *J. Phy. Org. Chem.* **2010**, *23*, 677-684.
(32) Pudney, C. R. J., L.; Sutcliffe, M. J.; Hay, S.; Scrutton N. S. : Direct Analysis of Donor-Acceptor Distance and Relationship to Isotope Effects and the Force Constant for Barrier Compression in Enzymatic H-Tunneling Reactions. *J. Am. Chem. Soc.* **2010**, *132*, 11329-11335.
(33) Klinman, J. P.; Offenbacher, A. R.: Understanding Biological Hydrogen Transfer Through the Lens of Temperature Dependent Kinetic Isotope Effects. *Acc. Chem. Res.* **2018**, *51*, 1966–1974.
(34) Truhlar, G. D.: Tunneling in enzymatic and nonenzymatic hydrogen transfer reactions. *J. Phy. Org. Chem.* **2010**, *23*, 660-676.
(35) Pang, J.; Pu, J.; Gao, J.; Truhlar, D. G.; Allemann, R. K.: Hydride Transfer Reaction Catalyzed by Hyperthermophilic Dihydrofolate Reductase Is Dominated by Quantum Mechanical Tunneling and Is Promoted by Both Inter- and Intramonomeric Correlated Motions. *J. Am. Chem. Soc.* **2006**, *128*, 8015-8023.
(36) Hatcher, E.; Soudackov, A. V.; Hammes-Schiffer, A.: Proton-Coupled Electron Transfer in Soybean Lipoxygenase: Dynamical Behavior and Temperature Dependence of Kinetic Isotope Effects. *J. Am. Chem. Soc.* **2007**, *129*, 187–196.
(37) Maharjan, B.; Raghibi Boroujeni, M.; Lefton, J.; White, O. R.; Razzaghi, M.; Hammann, B. A.; Derakhshani-Molayousefi, M.; Eilers, J. E.; Lu, Y.: Steric Effects on the Primary Isotope Dependence of Secondary Kinetic Isotope Effects in Hydride Transfer Reactions in Solution: Caused by the Isotopically Different Tunneling Ready State Conformations? *J. Am. Chem. Soc.* **2015**, *137*, 6653 - 6661.
(38) Ma, L.; Sakhaee, N.; Jafari, S.; Wilhelm, S.; Rahmani, P.; Lu, Y.: Imbalanced Transition States from α-H/D and Remote β-Type N-CH/D Secondary Kinetic Isotope Effects on the NADH/NAD+ Analogues in Their Hydride Tunneling Reactions in Solution. *J. Org. Chem.* **2019**, *84*, 5431–5439.
(39) Ghosh, S.; Saikh, F.; Das, J.; Pramanik, A. K.: Hantzsch 1,4-dihydropyridine synthesis in aqueous ethanol by visible light. *Tetrahedron Lett.* **2013**, *54*, 58-62.
(40) Zhu, X., -Q.; Zhang, M.-T.; Yu, A.; Wang, C.-H.; Cheng, J.-P.: Hydride, Hydrogen Atom, Proton, and Electron Transfer Driving Forces of Various Five-Membered Heterocyclic Organic Hydrides and Their Reaction Intermediates in Acetonitrile. *J. Am. Chem. Soc.* **2008**, *130*, 2501–2516.
(41) Bunting, J. W.: Merged Mechanisms for Hydride Transfer from 1,4-dihydropyridines. *Bioorg. Chem.* **1991**, *19*, 456-491.
(42) Lee, I.-S. H.; Jeoung, E. H.; Kreevoy, M. M.: Marcus Theory of a Parallel Effect on R for Hydride Transfer Reaction between NAD+ Analogues. *J Am Chem Soc* **1997**, *119*, 2722-2728.
(43) Lee, I.-S. H.; Jeoung, E. H.; Kreevoy, M. M.: Primary Kinetic Isotope Effects on Hydride Transfer from 1,3-Dimethyl-2-phenylbenzimidazoline to NAD+ Analogues. *J Am Chem Soc* **2001**, *123*, 7492-7496.
(44) Shen, G. B.; Xia, K.; Li, X. T.; Li, J. L.; Fu, Y. H.; Yuan, L.; Zhu, X. Q.: Prediction of Kinetic Isotope Effects for Various Hydride Transfer Reactions Using a New Kinetic Model. *J. Phys. Chem. A* **2016**, *120*, 1779−1799.
(45) Zhao, Y.; Truhlar, D. G.: The M06 Suite of Density Functionals for Main Group Thermochemistry, Thermochemical Kinetics, Noncovalent Interactions, Excited States, and Transition Elements: Two New Functionals and Systematic Testing of Four M06-Class Functionals and 12 Other Functionals. *Theor. Chem. Acc* **2008**, *120*, 215–241.
(46) Weigend, F.; Ahlrichs, R.: Balanced Basis Sets of Split Valence, Triple Zeta Valence and Quadruple Zeta Valence Quality for H to Rn: Design and Assessment of Accuracy. *Phys. Chem. Chem. Phys.* **2005**, *7*, 3297–3305.
(47) Marenich, A. V.; Cramer, C. J.; Truhlar, D. G.: Universal Solvation Model Based on Solute Electron Density and on a Continuum Model of the Solvent Defined by the Bulk Dielectric Constant and Atomic Surface Tensions. *J. Phys. Chem. B* **2009**, *113*, 6378–6396.
(48) Alecu, I. M.; Zheng, J.; Zhao, Y.; Truhlar, D. G.: Computational Thermochemistry: Scale Factor Databases and Scale Factors for Vibrational Frequencies Obtained from Electronic Model Chemistries. *J. Chem. Theory Comput.* **2010**, *6*, 2872–2887.
(49) Dunning, T. H.: Gaussian Basis Sets for Use in Correlated Molecular Calculations. I. The Atoms Boron through Neon and Hydrogen. *J. Chem. Phys.* **1989**, *90*, 1007–1023.
(50) Powell, M. F.; Bruice, T. C.: Effect of isotope scrambling and tunneling on the kinetic and product isotope effects for reduced nicotinamide adenine dinucleotide model hydride transfer reactions. *J. Am. Chem. Soc.* **1983**, *105*, 7139–7149.
(51) Lu, Y.; Zhao, Y.; Handoo, K. L.; Parker, V. D.: Hydride-exchange reactions between NADH and NAD+ model compounds under non-steady-state conditions. Apparent and Real kinetic isotope effects. *Org. Biomol. Chem.* **2003**, *1*, 173 - 181.
(52) Watt, C. I. F.: Primary kinetic hydrogen isotope effects in deprotonations of carbon acids. *J. Phy. Org. Chem.* **2010**, *23*, 561-571.
(53) Liu, Q.; Zhao, Y.; Hammann, B.; Eilers, J.; Lu, Y.; Kohen, A.: A Model Reaction Assesses Contribution of H-Tunneling and Coupled Motions to Enzyme Catalysis. *J. Org. Chem.* **2012**, *77*, 6825–6833.
(54) Brown, H. C.; McDonald, G. J.: Secondary Isotope Effects in the Reactions of Methyl-d3-pyridines with Alkyl Iodides. Evidence for a Smaller Steric Requirement of the Methyl-d3 over the Methyl-d0 Group. *J. Am. Chem. Soc.* **1966**, *88*, 2514 - 2519.
(55) Hayama, T.; Baldridge, K. K.; Wu, Y.-T.; Linden, A.; Siegel, J. S.: Steric Isotope Effects Gauged by the Bowl-Inversion Barrier in Selectively Deuterated Pentaarylcorannulenes. *J. Am. Chem. Soc.* **2008**, *130*, 1583-1591.
(56) Hammann, B.; Razzaghi, M.; Kashefolgheta, S.; Lu, Y.: Imbalanced Tunneling Ready States in Alcohol Dehydrogenase Model Reactions: Rehybridization Lags behind H-Tunneling. *Chem Comm* **2012**, *48*, 11337-11339.
(57) Hermes, J. D.; Cleland, W. W.: Evidence from multiple isotope effect determinations for coupled hydrogen motion and tunneling in the reaction catalyzed by glucose-6-phosphate dehydrogenase. *J. Am. Chem. Soc.* **1984**, *106*, 7263-7264.
(58) Cook, P. F.; Oppenheimer, N. J.; Cleland, W. W.: Secondary deuterium and nitrogen- 15 isotope effects in enzyme-catalyzed reactions. Chemical mechanism of liver alcohol dehydrogenase. *Biochemistry* **1981**, *20*, 1817-1825.
(59) Huskey, W. P.; Schowen, R. L.: Reaction-coordinate tunneling in hydride transfer reactions. *J. Am. Chem. Soc.* **1983**, *105*, 5704-5706.
(60) Cha, Y.; Murray, C. J.; Klinman, J. P.: Hydrogen tunneling in enzyme reactions. *Science* **1989**, *243*, 1325-1330.
(61) Rucker, J.; Klinman, J. P.: Computational study of tunneling and coupled motion. *J. Am. Chem. Soc.* **1999**, *121*, 1997-2006.
(62) Roston, D.; Kohen, A.: A Critical Test of the "Tunneling and Coupled Motion" Concept in Enzymatic Alcohol Oxidation. *J. Am. Chem. Soc.* **2013**, *135*, 13624–13627.
(63) Derakhshani-Molayousefi, M.; Kashefolgheta, S.; Eilers, J. E.; Lu, Y.: Computational Replication of the Primary Isotope Dependence of Secondary Kinetic Isotope Effects in Solution Hydride-Transfer Reactions: Supporting the Isotopically Different Tunneling Ready State Conformations. *J. Phys. Chem. A* **2016**, *120*, 4277−4284.
(64) Wilde, T. C.; Blotny, G.; Pollack, R. M.: Experimental Evidence for Enzyme-Enhanced Coupled Motion/Quantum Mechanical Hydrogen Tunneling by Ketosteroid Isomerase. *J. Am. Chem. Soc.* **2008**, *130*, 6577–6585.
(65) Pu, J.; Ma, S.; Garcia-Viloca, M.; Gao, J.; Truhlar, D. J.; Kohen, A.: Nonperfect Synchronization of Reaction Center Rehybridization in the Transition State of the Hydride Transfer Catalyzed by Dihydrofolate Reductase. *J. Am. Chem. Soc.* **2005**, *127*, 14879-14886.
(66) Zhu, X. Q.; Deng, F. H.; Yang, J. D.; Li, X. T.; Chen, Q.; Lei, N. P.; Meng, F. K.; Zhao, X. P.; Han, S. H.; Hao, E. J.; Mu, Y. Y.: A classical but new kinetic equation for hydride transfer reactions. *Org. Biomol. Chem.*

2013, *11*, 6071-6089.
(67) Melander, L.; Saunders, W. H.: Reaction rates of isotopic molecules. In *Reaction Rates of Isotopic Molecules*; 4th ed.; Krieger, R. E.: Malabar, FL, 1987; pp 170-201.
(68) Bell, R. P.: *The tunnel effect in chemistry*; Chapman & Hall: London & New York., 1980.
(69) Stojković, V.; Kohen, A.: Enzymatic H-transfer: Quantum tunneling and coupled motion from kinetic isotope effects. *Isr. J. Chem.* **2009**, *49*, 163-173.
(70) Sharma, S. C.; Klinman, J. P.: Experimental Evidence for Hydrogen Tunneling when the Isotopic Arrhenius Prefactor (AH/AD) is Unity. *J. Am. Chem. Soc.* **2008**, *130*, 17632–17633.
(71) Yasuia, S.; Ohno, A.: Model studies wić nicotinamide derivatives. *Bioorg. Chem.* **1986**, *14*, 70-96.
(72) Fukuzumi, S.; Ohkubo, K.; Tokuda, Y.; Suenobu, T.: Hydride Transfer from 9-Substituted 10-Methyl-9,10-dihydroacridines to Hydride Acceptors via Charge-Transfer Complexes and Sequential Electron-Proton-Electron Transfer. A Negative Temperature Dependence of the Rates. *J. Am. Chem. Soc.* **2000**, *122*, 4286-4294.
(73) Lu, Y.; Zhao, Y.; Parker, V. D.: Proton-transfer reactions of methylarene radical cations with pyridine bases under non-steady-state conditions. Real kinetic isotope effect evidence for extensive tunneling. *J Am. Chem. Soc.* **2001**, *123*, 5900-5907.
(74) Zhang, J.; Klinman, J. P.: Enzymatic Methyl Transfer: Role of an Active Site Residue in Generating Active Site Compaction That Correlates with Catalytic Efficiency. *J. Am. Chem. Soc.* **2011**, *133*, 17134−17137.
(75) Zhang, J.; Klinman, J. P.: Convergent Mechanistic Features between the Structurally Diverse N- and O-Methyltransferases: Glycine N-Methyltransferase and Catechol O-Methyltransferase. *J. Am. Chem. Soc.* **2016**, *138*, 9158-9165.
(76) Kohen, A.: Kinetic isotope effects as probes for hydrogen tunneling in enzyme catalysis. In *Isotope effects in chemistry and biology*; Kohen, A., Limbach, H. H., Eds.; Taylor & Francis, CRC Press: Boca Raton, FL, 2006; Vol. Ch. 28; pp 743-764.
(77) Kim, Y.; Kreevoy, M. M.: The experimental manifestations of corner-cutting tunneling. *J. Am. Chem. Soc.* **1992**, *114*, 7116-7123.
(78) Horitani, M.; Offenbacher, A. R.; Carr, C. A. M.; Yu, T.; Hoeke, V.; Cutsail, G. E.; Hammes-Schiffer, S.; Klinman, J. P.; Hoffman, B. M.: C-13 ENDOR Spectroscopy of Lipoxygenase-Substrate Complexes Reveals the Structural Basis for C-H Activation by Tunneling. *J. Am. Chem. Soc.* **2017**, *139*, 1984−1997.
(79) Gready, J. E.: Theoretical Studies on the Activation of the Pterin Cofactor in the Catalytic Mechanism of Dihydrofolate Reductase1. *Biochemistry* **1985**, *24*, 4761-4766.
(80) Stojković, V.; Perissinotti, L. L.; Lee, J.; Benkovic, S. J.; Kohen, A.: The effect of active-site isoleucine to alanine mutation on the DHFR catalyzed H-transfer. *Chem. Comm.* **2010**, *46*, 8974 - 8976.
(81) Kuznetsov, A. M.; Ulstrup, J.: Proton and hydrogen atom tunneling in hydrolytic and redox enzyme catalysis. *Can. J. Chem.* **1999**, *77*, 1085-1096.
(82) Du, M. R.; Borreguero, J. M.; Cuneo, M. J.; Ramanathan, A.; He, J.; Kamath, G.; Chennubhotla, S. C.; Meilleur, F.; Howell, E. E.; Herwig, K. W.; Myles, D. A. A.; Agarwal, P. K.: Modulating Enzyme Activity by Altering Protein Dynamics with Solvent. *Biochemistry* **2018**, *57*, 4263−4275.
(83) Wisłocka, Ż.; Nowak, I.; Jarczewski, A.: Kinetic study of the proton transfer reaction between 1-nitro-1-(4-nitrophenyl)alkanes and P1-t-Bu phosphazene base in THF solvent. *J. Mol. Struct.* **2006**, *788*, 152-158.

Graphical Table of Contents